2008 American Control Conference
Westin Seattle Hotel, Seattle, Washington, USA
June 11-13, 2008

Frequency Domain Analysis and Design of Iterative Learning Control for Systems with Stochastic Disturbances

D.A. Bristow

Abstract—**In this work we examine the performance of Iterative Learning Control (ILC) for systems with non-repeating disturbances and random noise. Single-input, single-output linear time-invariant systems and iteration-invariant learning filters are considered. We find that a tradeoff exists between the convergence rate and converged error spectrum. Optimal filter designs, which are dependant on the disturbance and noise spectra, are developed. We also present simple design guidelines for the case when explicit models of disturbance and noise spectra are not available. A numerical design example is presented.**

I. Introduction

ITERATIVE learning control (ILC) [1]-[3] is used to improve the performance of systems that repeat the same operation many times. ILC uses the tracking errors from previous iterations of the repeated motion to generate a feedforward control signal for subsequent iterations. Convergence of the learning process results in a feedforward control signal that is customized for the repeated motion, typically yielding very low tracking error.

One of the standard assumptions in ILC is that input signals repeat [1], although in all physical implementations measurement signals are subject to random noise and the system may be affected by random disturbances. Several specialized learning algorithms [4]-[7] have been developed in recent years for systems with stochastic disturbances. These learning algorithms provide asymptotic noise and non-repeating disturbance insensitivity, but rely on an iteration-varying and decaying learning filter. Most applications of ILC, however, use simpler iteration-invariant learning filters. Furthermore, decaying learning filters also decrease adaptability of the ILC to changes in deterministic disturbances that occur after initial convergence.

In this work we examine the sensitivity of iteration-invariant learning filters to mixed deterministic and stochastic disturbances for discrete-time (DT), single-input, single-output (SISO), linear time-invariant (LTI) systems. We show that there is a tradeoff between convergence rate and converged error spectrum where fast convergence results in largest error, while slow convergence results in smallest error. Optimal learning filters that minimize converged error for a desired convergence designs are obtained. The optimal filters are functions of the deterministic and stochastic disturbance and noise spectra. Because it may be undesirable in some applications to accurately model and identify these spectra, simple design guidelines are also presented. Finally, a numerical example is presented to demonstrate the optimal filter design.

The remainder of this paper is organized as follows. In Section II the problem setup is given with system and signal descriptions. In Section III convergence and performance results are developed. Optimal filter design is presented in Section IV. Extensions and simple design guidelines are presented in Section V. A numerical example is given and Section VI and conclusions are given in Section VII.

This work was supported in part by the University of Illinois at Urbana-Champaign Nano-CEMMS center NSF Award #0328162.

D.A. Bristow is with the Department of Mechanical and Aerospace Engineering, Missouri University of Science and Technology, Rolla, MO.

II. System Description

We are interested in deriving frequency-domain results and therefore assume that our system operates on an infinite time horizon. Consider the LTI, SISO DT system given by,

$$e_j(k) = -P(\mathrm{q})u_j(k) + d(k) + w_j(k) \tag{1}$$

where $k = 0,1,\ldots$ is the time index, $j = 0,1,\ldots$ is the iteration index, q is the forward time-shift operator $\mathrm{q}x(k) = x(k+1)$, q^{-1} is the backward time-shift operator $\mathrm{q}^{-1}x(k) = x(k-1)$, u is the control input, e is the error, d is a deterministic signal, w is a stationary random disturbance, and P is a stable system. Iteration-invariant (II) disturbances [8] and II initial conditions [9] can be captured in $d(k)$. We assume that the error measurement, $\hat{e}_j(k)$, is corrupted by noise as,

$$\hat{e}_j(k) = e_j(k) + v_j(k), \tag{2}$$

where v is stationary random noise. Consider the first-order ILC algorithm,

$$u_{j+1}(k) = Q(\mathrm{q})\left[u_j(k) + L(\mathrm{q})\hat{e}_j(k)\right]. \tag{3}$$

A diagram of the complete system is shown in Figure 1. We assume the following:

A1) $u_0(k) = 0$.

A2) $|d(k)| \le M$.

A3) $\mathrm{E}\left[w_{j_1}(k_1)v_{j_2}(k_2)\right] = 0$ for all j_1, j_2, k_1, k_2.

A4) $\mathrm{E}\left[w_{j_1}(k_1)w_{j_2}(k_2)\right] = 0$, $\mathrm{E}\left[v_{j_1}(k_1)v_{j_2}(k_2)\right] = 0$, $\mathrm{E}\left[w_{j_1}(k_1)d(k_2)\right] = 0$, $\mathrm{E}\left[v_{j_1}(k_1)d(k_2)\right] = 0$, for $j_1 \neq j_2$ and all k_1, k_2.

A5) $P(\mathrm{q})$ is a rational function with relative degree 0.

Assumption A5 can be relaxed to include systems with nonzero relative degree. In the case of relative degree, $m \neq 0$, the control signal can be shifted left by *m* samples so that the sequence of control inputs is $\{u_j(-m), u_j(1-m), u_j(2-m), \ldots\}$. That is, we replace $u_j(k)$ in (1) with $u_j(k-m)$ so that we have,

$$e_j(k) = -P(\mathrm{q})u_j(k-m) + d(k) + w_j(k). \tag{4}$$

We then define a 'new' plant, $P_{new}(\mathrm{q}) = \mathrm{q}^m P(\mathrm{q})$, which has zero relative degree and results in

$$e_j(k) = -P_{new}(\mathrm{q})u_j(k) + d(k) + w_j(k). \tag{5}$$

This process is possible in ILC because the entire sequence of control inputs for iteration *j* is calculated before the iteration begins. Therefore, it does not violate causality to apply the control sequence *m* time steps early.

In this work we are primarily interested in signal spectra. We define the spectrum of a signal, $s(t)$, as,

$$\Phi_s(\omega) = \sum_{\tau=-\infty}^{\infty} R_s(\tau) e^{-i\omega\tau}, \tag{6}$$

where,

$$R_s(\tau) = \sum_{t=0}^{\infty} E\left[s(t)s(t+\tau)\right], \tag{7}$$

is the autocorrelation.

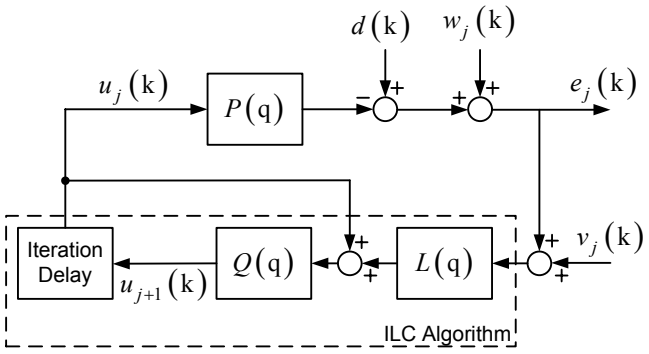

Fig. 1. Diagram of iterative learning control system.

III. Convergence and Performance

In this section we obtain the power spectrum of the asymptotic error, as well as sufficient conditions for its convergence, and the iteration-domain convergence rate. We begin by deriving the closed-loop 2-dimensional system by rewriting (1) as,

$$P(\mathrm{q})u_j(k) = -e_j(k) + d(k) + w_j(k), \tag{8}$$

multiplying (3) by *P*,

$$\begin{aligned} P(\mathrm{q})u_{j+1}(k) = Q(\mathrm{q})\big[&P(\mathrm{q})u_j(k) \\ &+ L(\mathrm{q})P(\mathrm{q})e_j(k) + L(\mathrm{q})P(\mathrm{q})v_j(k)\big], \end{aligned} \tag{9}$$

and substituting (8) into (9) yielding,

$$\begin{aligned} e_j(k) = {} & Q(\mathrm{q})\big[1 - L(\mathrm{q})P(\mathrm{q})\big]e_{j-1}(k) \\ & + \big(1 - Q(\mathrm{q})\big)d(k) + w_j(k) - Q(\mathrm{q})w_{j-1}(k) \\ & - Q(\mathrm{q})L(\mathrm{q})P(\mathrm{q})v_{j-1}(k). \end{aligned} \tag{10}$$

We cannot find the power spectrum of e_j from the recursive solution in (10) because e_{j-1} is correlated with w_{j-1}. Therefore, we first find the nonrecursive solution to (10) as,

$$\begin{aligned} e_j(k) = {} & X_j(\mathrm{q})d(k) \\ & + \sum_{r=0}^{j-1} Y_r(\mathrm{q})\big(w_{j-1-r}(k) + v_{j-1-r}(k)\big) + w_j(k), \end{aligned} \tag{11}$$

for $j \geq 1$, where

$$\begin{aligned} X_j(\mathrm{q}) = {} & \big[Q(\mathrm{q})\big(1 - L(\mathrm{q})P(\mathrm{q})\big)\big]^j \\ & + \sum_{r=0}^{j-1} \big[Q(\mathrm{q})\big(1 - L(\mathrm{q})P(\mathrm{q})\big)\big]^r \big(1 - Q(\mathrm{q})\big), \\ Y_r(\mathrm{q}) = {} & -\big[Q(\mathrm{q})\big(1 - L(\mathrm{q})P(\mathrm{q})\big)\big]^r Q(\mathrm{q})L(\mathrm{q})P(\mathrm{q}). \end{aligned} \tag{12}$$

The nonrecursive solution (11), (12) can be verified by substituting into (10). The verification is omitted here due to space constraints. A block diagram of the nonrecursive solution is shown in Figure 2.

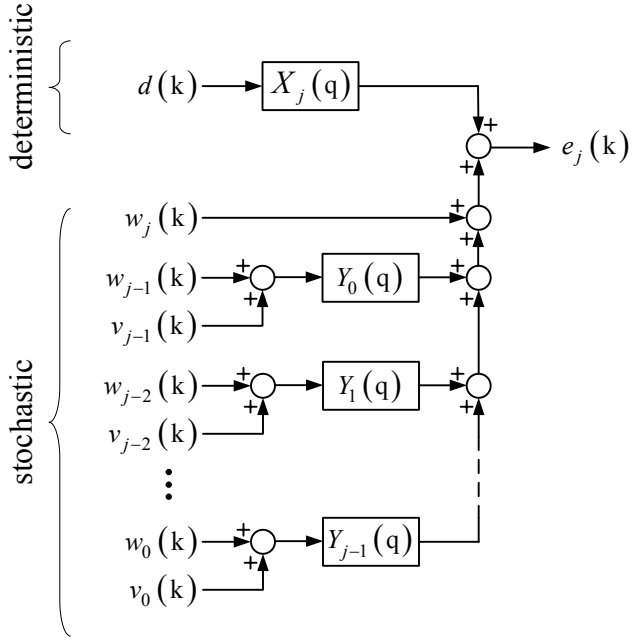

Fig. 2. Block diagram for the nonrecursive solution.

From (11), (12) we can now find the power spectrum of the error for the j^{th} iteration as,

$$\begin{aligned} \Phi_{e_j}(\omega) = {} & \left|X_j\left(e^{i\omega}\right)\right|^2 \Phi_d(\omega) \\ & + \sum_{r=0}^{j-1} \left|Y_r\left(e^{i\omega}\right)\right|^2 \left(\Phi_w(\omega) + \Phi_v(\omega)\right) + \Phi_w(\omega). \end{aligned} \tag{13}$$

Theorem 1: If

$$\max_{\omega\in[-\pi,\pi]} \left|Q\left(e^{i\omega}\right)\left[1 - L\left(e^{i\omega}\right)P\left(e^{i\omega}\right)\right]\right| < 1, \tag{14}$$

then the error power spectrum converges and,

$$\Phi_{e_\infty}(\omega) \triangleq \lim_{j\to\infty}\Phi_{e_j}(\omega)$$
$$= \frac{\left|1-Q\left(e^{i\omega}\right)\right|^2}{\left|1-Q\left(e^{i\omega}\right)\left[1-L\left(e^{i\omega}\right)P\left(e^{i\omega}\right)\right]\right|^2}\Phi_d(\omega)+\Phi_w(\omega) \quad (15)$$
$$+\frac{\left|Q\left(e^{i\omega}\right)L\left(e^{i\omega}\right)P\left(e^{i\omega}\right)\right|^2}{1-\left|Q\left(e^{i\omega}\right)\left[1-L\left(e^{i\omega}\right)P\left(e^{i\omega}\right)\right]\right|^2}\left(\Phi_w(\omega)+\Phi_v(\omega)\right).$$

Proof: For compactness in the following, we drop the frequency arguments, but note that the argument for systems is $e^{i\omega}$ and the argument for signal spectra is ω. Let $A = Q[1-LP]$. From (12),(13),

$$\lim_{j\to\infty}\Phi_{e_j} = \lim_{j\to\infty}\left|A^j+\sum_{r=0}^{j-1}A^r(1-Q)\right|^2\Phi_d$$
$$+\lim_{j\to\infty}\sum_{r=0}^{j-1}\left|A^rQPL\right|^2\left(\Phi_w+\Phi_v\right)+\Phi_w,$$
$$=\lim_{j\to\infty}\left[\left|A^j\right|^2+2\left|A^j\right|\left|\sum_{r=0}^{j-1}A^r(1-Q)\right|\cos\theta_j\right.$$
$$\left.+\left|\sum_{r=0}^{j-1}A^r(1-Q)\right|^2\right]\Phi_d$$
$$+\lim_{j\to\infty}\left[\sum_{r=0}^{j-1}\left|A^rQPL\right|^2\right]\left(\Phi_w+\Phi_v\right)+\Phi_w,$$
$$=\lim_{j\to\infty}\left|A^j\right|^2\Phi_d+\lim_{j\to\infty}2\left|A^j\right|\left|\sum_{r=0}^{j-1}A^r\right|\left|1-Q\right|\cos\left(\theta_j\right)\Phi_d$$
$$+\lim_{j\to\infty}\left|\sum_{r=0}^{j-1}A^r\right|^2\left|1-Q\right|^2\Phi_d$$
$$+\lim_{j\to\infty}\sum_{r=0}^{j-1}\left|A^r\right|^2\left|QPL\right|^2\left(\Phi_w+\Phi_v\right)+\Phi_w.$$

where $\theta_j = \angle A^j - \angle\sum_{r=0}^{j-1}A^r(1-Q)$. If (14), then,

$$\lim_{j\to\infty}\left|A^j\right|^2 = 0,$$
$$\lim_{j\to\infty}\left|\sum_{r=0}^{j-1}A^r\right| = \frac{1}{|1-A|},$$
$$\lim_{j\to\infty}\sum_{r=0}^{j-1}\left|A^r\right|^2 = \frac{1}{1-|A|},$$

and (15) follows. □

The necessary condition for convergence of the power spectrum, (14), is the familiar frequency-domain stability condition for ILC [1],[9]. In the following, we show that this condition is also related to the convergence rate of the spectrum.

By convention, we set $w_j(k) = v_j(k) = 0$ to find the convergence rate. We assume convergence, and thus the asymptotic error can be found from (10) as

$$\hat{e}_\infty(k) \triangleq \lim_{j\to\infty}e_j(k)$$
$$= \frac{1-Q(\mathrm{q})}{1-Q(\mathrm{q})\left(1-L(\mathrm{q})P(\mathrm{q})\right)}d(k). \quad (16)$$

Let $\Phi_{\hat{e}_\infty - e_j}(\omega)$ be the power spectrum of $\hat{e}_\infty(k) - e_j(k)$.

Definition 1: The convergence rate of the system (1), (3) with $w_j(k) = v_j(k) = 0$ is the smallest γ such that

$$\Phi_{\hat{e}_\infty - e_{j+1}}(\omega) \le \gamma\Phi_{\hat{e}_\infty - e_j}(\omega) \text{ for all } \omega\in[-\pi,\pi]. \quad (17)$$

From (10) and (16), one can verify that,

$$\gamma = \max_{\omega\in[-\pi,\pi]}\left|Q\left(e^{i\omega}\right)\left[1-P\left(e^{i\omega}\right)L\left(e^{i\omega}\right)\right]\right|^2 \quad (18)$$

and, from (14) we find that $0 \le \gamma < 1$ for stability.

IV. Optimal Gains for Model-Inversion ILC

Here we consider the class of model-inversion learning functions,

$$L\left(e^{i\omega}\right) = \eta(\omega)P^{-1}\left(e^{i\omega}\right), \quad (19)$$

where $\eta\in\mathbb{R}$ is the inversion gain. To simplify the analysis in this section, we write $Q\left(e^{i\omega}\right)$ in its Euler form,

$$Q\left(e^{i\omega}\right) = \xi(\omega)e^{i\phi(\omega)}, \quad (20)$$

where $\xi,\phi\in\mathbb{R}$, $\xi\ge 0$ and $-\pi\ge\phi\ge\pi$. Then from (15),

$$\Phi_{e_\infty}(\omega) = \frac{\left|1-\xi(\omega)e^{i\phi(\omega)}\right|^2}{\left|1-\xi(\omega)e^{i\phi(\omega)}\left(1-\eta(\omega)\right)\right|^2}\Phi_d(\omega)+\Phi_w(\omega)$$
$$+\frac{\left|\xi(\omega)\eta(\omega)\right|^2}{1-\left|\xi(\omega)\left(1-\eta(\omega)\right)\right|^2}\left(\Phi_w(\omega)+\Phi_v(\omega)\right). \quad (21)$$

We are interested in determining the best filter design (i.e. $\eta^*(\omega)$, $\xi^*(\omega)$, and $\phi^*(\omega)$) that will minimize the asymptotic power spectrum (15). However, the results in this section will show that, as we approach the minimum asymptotic power spectrum, the convergence rate approaches 1 (very slow convergence). Thus, we will find a tradeoff between asymptotic performance and convergence rate. For practical reasons we specify an upper bound on the convergence rate to ensure that approximate convergence occurs in a reasonable number of iterations. We pose this problem as the following optimal design problem.

Optimal Design Problem

Given the ILC system (1), (3) with model-inversion learning (19), and maximum desired convergence rate $\bar{\gamma}$, find $\eta^*(\omega)$, $\xi^*(\omega)$, and $\phi^*(\omega)$ that solve

$$\min_{\eta,\xi,\phi}\Phi_{e_\infty}(\omega) \text{ such that } \gamma\le\bar{\gamma}<1. \quad (22)$$

We solve the above optimal design problem in two steps. Theorem 2 gives the solution for $\Phi_d(\omega)\ne 0$ and

Theorem 3 gives the solution for $\Phi_d(\omega)=0$.

Theorem 2: If $\Phi_d(\omega)\neq 0$,

$$\min_{\substack{\eta(\omega),\xi(\omega),\phi(\omega)\\ \gamma(\omega)\le\overline{\gamma}<1}}\Phi_{e_\infty}(\omega) = \frac{\left(1-\overline{\gamma}^{1/2}\right)\Phi_d(\omega)\left(\Phi_w+\Phi_v\right)}{\left(1+\overline{\gamma}^{1/2}\right)\Phi_d(\omega)+\left(1-\overline{\gamma}^{1/2}\right)\left(\Phi_w+\Phi_v\right)}+\Phi_w(\omega) \tag{23}$$

which is achieved by,

$$\eta^*(\omega)=\frac{\left(1-\overline{\gamma}\right)\Phi_d(\omega)}{\left(1+\overline{\gamma}^{1/2}\right)\Phi_d(\omega)+\overline{\gamma}^{1/2}\left(1-\overline{\gamma}^{1/2}\right)\left(\Phi_w(\omega)+\Phi_v(\omega)\right)}, \tag{24}$$

$$\xi^*(\omega)=\frac{\left(1+\overline{\gamma}^{1/2}\right)\Phi_d(\omega)+\overline{\gamma}^{1/2}\left(1-\overline{\gamma}^{1/2}\right)\left(\Phi_w(\omega)+\Phi_v(\omega)\right)}{\left(1+\overline{\gamma}^{1/2}\right)\Phi_d(\omega)+\left(1-\overline{\gamma}^{1/2}\right)\left(\Phi_w(\omega)+\Phi_v(\omega)\right)}, \tag{25}$$

$$\phi^*(\omega)=0, \tag{26}$$

with convergence rate $\gamma^*=\overline{\gamma}$.

Proof: Again, for compactness, we will drop the frequency arguments. Assume $\xi\neq 0$ and use the change of variables, $\eta=1-c/\xi$. We have that $\left|Q(1-LP)\right|=\left|\xi(1-\eta)\right|=|c|$ and therefore, from (18), $|c|=\gamma^{1/2}$. Thus, the convergence rate constraint is a constraint on c,

$$|c|\le\overline{\gamma}^{1/2}.$$

With the change of variables,

$$\Phi_{e_\infty}=\frac{\left|1-\xi e^{i\phi}\right|^2}{\left|1-ce^{i\phi}\right|^2}\Phi_d+\frac{|\xi-c|^2}{1-c^2}\left(\Phi_w+\Phi_v\right)+\Phi_w.$$

We first solve for ϕ^* by solving $\partial\Phi_{e_\infty}/\partial\phi\big|_{\phi=\phi^*}=0$ as,

$$\frac{\partial}{\partial\phi}\frac{\left|1-\xi e^{i\phi}\right|^2}{\left|1-\xi e^{i\phi}(1-\eta)\right|^2}\Phi_d=0,$$

$$\frac{\partial}{\partial\phi}\frac{1-2\xi\cos\phi+\xi^2}{1-2\xi(1-\eta)\cos\phi+\xi^2(1-\eta)^2}\Phi_d=0,$$

$$\frac{\begin{pmatrix}2\xi\left[1-2\xi(1-\eta)\cos\phi+\xi^2(1-\eta)^2\right]\sin\phi\\ -2\xi(1-\eta)\left[1-2\xi\cos\phi+\xi^2\right]\sin\phi\end{pmatrix}}{\left[1-2\xi(1-\eta)\cos\phi+\xi^2(1-\eta)^2\right]^2}=0,$$

$$\frac{2\xi\eta\left[1+\xi^2(\eta-1)\right]\sin\phi}{\left[1-2\xi(1-\eta)\cos\phi+\xi^2(1-\eta)^2\right]^2}=0,$$

$$\phi^*=0.$$

We then have,

$$\Phi_{e_\infty}=\frac{(1-\xi)^2}{(1-c)^2}\Phi_d+\frac{(\xi-c)^2}{(1-c)(1+c)}\left(\Phi_w+\Phi_v\right)+\Phi_w.$$

We find ξ^* by solving $\partial\Phi_{e_\infty}/\partial\xi\big|_{\xi=\xi^*}=0$ as,

$$0=\frac{2(\xi^*-1)}{(1-c)^2}\Phi_d+\frac{2(\xi^*-c)}{(1-c)(1+c)}\left(\Phi_w+\Phi_v\right),$$

$$0=(\xi^*-1)(1+c)\Phi_d+(\xi^*-c)(1-c)\left(\Phi_w+\Phi_v\right),$$

$$\xi^*=\frac{(1+c)\Phi_d+c(1-c)\left(\Phi_w+\Phi_v\right)}{(1+c)\Phi_d+(1-c)\left(\Phi_w+\Phi_v\right)}.$$

Then,

$$\begin{aligned}\Phi_{e_\infty}&=\frac{\left(1-\frac{(1+c)\Phi_d+c(1-c)\left(\Phi_w+\Phi_v\right)}{(1+c)\Phi_d+(1-c)\left(\Phi_w+\Phi_v\right)}\right)^2}{(1-c)^2}\Phi_d\\&\quad+\frac{\left(\frac{(1+c)\Phi_d+c(1-c)\left(\Phi_w+\Phi_v\right)}{(1+c)\Phi_d+(1-c)\left(\Phi_w+\Phi_v\right)}-c\right)^2}{(1-c)(1+c)}\\&\quad\cdot\left(\Phi_w+\Phi_v\right)+\Phi_w,\\&=\frac{(1-c)^2\left(\Phi_w+\Phi_v\right)^2}{\left[(1+c)\Phi_d+(1-c)\left(\Phi_w+\Phi_v\right)\right]^2}\Phi_d\\&\quad+\frac{\left(1-c^2\right)\Phi_d^2}{\left[(1+c)\Phi_d+(1-c)\left(\Phi_w+\Phi_v\right)\right]^2}\left(\Phi_w+\Phi_v\right)+\Phi_w,\\&=\frac{(1-c)\Phi_d\left(\Phi_w+\Phi_v\right)}{(1+c)\Phi_d+(1-c)\left(\Phi_w+\Phi_v\right)}+\Phi_w.\end{aligned}$$

Now,

$$\frac{\partial\Phi_{e_\infty}}{\partial c}=\frac{(1-c)\Phi_d\left(\Phi_w+\Phi_v\right)}{(1+c)\Phi_d+(1-c)\left(\Phi_w+\Phi_v\right)},$$

$$=\frac{\begin{pmatrix}-\left[(1+c)\Phi_d+(1-c)\left(\Phi_w+\Phi_v\right)\right]\Phi_d\left(\Phi_w+\Phi_v\right)\\ -(1-c)\Phi_d\left(\Phi_w+\Phi_v\right)\left[\Phi_d-\left(\Phi_w+\Phi_v\right)\right]\end{pmatrix}}{(1+c)\Phi_d+(1-c)\left(\Phi_w+\Phi_v\right)},$$

$$=\frac{\begin{pmatrix}-(1+c)\Phi_d^2\left(\Phi_w+\Phi_v\right)-(1-c)\Phi_d\left(\Phi_w+\Phi_v\right)^2\\ -(1-c)\Phi_d^2\left(\Phi_w+\Phi_v\right)+(1-c)\Phi_d\left(\Phi_w+\Phi_v\right)^2\end{pmatrix}}{(1+c)\Phi_d+(1-c)\left(\Phi_w+\Phi_v\right)},$$

$$=\frac{-2\Phi_d^2\left(\Phi_w+\Phi_v\right)+2c\Phi_d\left(\Phi_w+\Phi_v\right)^2}{(1+c)\Phi_d+(1-c)\left(\Phi_w+\Phi_v\right)}.$$

Recall the constraint $|c|\le\overline{\gamma}^{1/2}<1$. Therefore, $\partial\Phi_{e_\infty}/\partial c<0$ for $|c|\le\overline{\gamma}^{1/2}$ and hence the optimal lies on the constraint,

$$c^*=\overline{\gamma}^{1/2}.$$

With the appropriate substitutions, we have arrived at (23)-(26).

Now, assume that $\xi^*=0$. Then, $\Phi_{e_\infty}=\Phi_d+\Phi_w$, which

is always larger than (23) for $\Phi_d(\omega) \neq 0$, so the optimal solution must be (23)-(26). □

Remark 1: As discussed earlier, there is a tradeoff between the asymptotic error and the convergence rate. From Theorem 2 we find that the minimum spectrum is obtained when the convergence rate approaches 1 (very slow convergence), $\lim_{\bar{\gamma}\to 1} \Phi^*_{e_\infty}(\omega) = \Phi_w(\omega)$. The minimum is $\Phi_w(\omega)$ because w_j adds directly to the error, as shown in Figure 2. The best that can be done is for ILC to be insensitive to the random disturbances and noise from previous iterations, through the $Y_r(\mathrm{q})$ terms.

Remark 2: It has been a long-held belief that zero-phase filters for *Q* provide the best performance [10],[11]. To the authors' best knowledge, the result in Theorem 2 is the first proof of their optimality.

For completeness, the following theorem obtains the optimal ILC for $\Phi_d(\omega) = 0$. That is, the case where there input signals have no repeatable component.

Theorem 3: If $\Phi_d(\omega) = 0$,

$$\min_{\substack{\eta(\omega),\xi(\omega),\phi(\omega)\\ \gamma(\omega)\le\bar{\gamma}<1}} \Phi_{e_\infty}(\omega) = \Phi_w(\omega), \tag{27}$$

which is achieved by,

$$\xi^*(\omega) = 0, \tag{28}$$

with convergence rate $\gamma^* = 0$.

Proof: From (21) we have,

$$\Phi_{e_\infty} = \frac{|\xi\eta|^2}{1-|\xi(1-\eta)|^2}(\Phi_w + \Phi_v) + \Phi_w \geq \Phi_w$$

because $|\xi(1-\eta)|^2 = \gamma < 1$. Clearly, $\xi^* = 0$ gives the minimum with convergence rate $\gamma^* = 0$. □

As expected, Theorem 3 verifies that when the input signal has no repeated component, the best performance is obtained when the ILC is disabled, or $\xi^*(\omega) = 0$.

Using the results of the above theorems we can construct the noise sensitivity plot in Figure 3. As discussed in Remark 1, noise sensitivity of the optimal ILC decreases with increasing convergence rate (slow learning). It is worth noting that the spectrum for the 0th iteration, without ILC, is $\Phi_d + \Phi_w$. Therefore, performance always improves using the optimal gains, as we might expect, but the performance improvement depends on the signal-to-noise ratio *and* desired convergence rate. Figure 3 shows that given any desired performance level $\Phi^{desired}_{e_\infty} > \Phi_w$, one can always find a sufficiently slow convergence rate that meets or exceeds it.

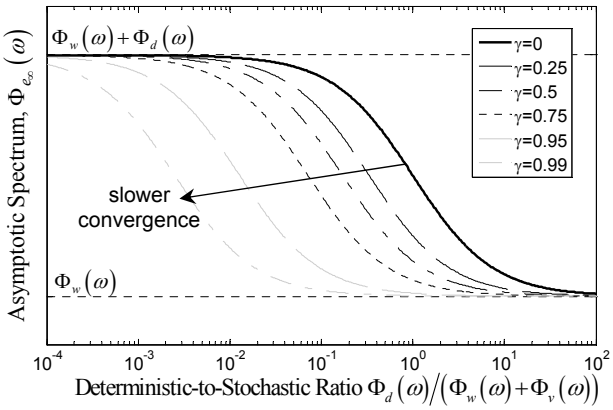

Fig. 3. Noise sensitivity of the optimal ILC (23)-(26).

V. Extensions

In this section we consider extensions of the previous results to several issues of practical importance. These include model uncertainty robustness, finite length iterations, and filter construction.

A. Model Uncertainty Robustness

Using standard techniques [9],[12], the above results can be easily extended to provide robust stability for plants with frequency-domain bounded uncertainty

$$|P(e^{i\omega})| < |\bar{P}(e^{i\omega})|.$$

Recall the sufficient stability condition (14), rewritten here using the optimal results from Theorem 2,

$$\max_{\omega\in[-\pi,\pi]} \left|\xi^*(\omega)\left[1-\eta^*(\omega)\hat{P}^{-1}(e^{i\omega})P(e^{i\omega})\right]\right| < 1,$$

where $\hat{P}(e^{i\omega})$ is a model of the bounded uncertain system. Equivalently, the sufficient stability condition can be written as,

$$|\xi^*(\omega)| < \frac{1}{\left|1-\eta^*(\omega)\hat{P}^{-1}(e^{i\omega})P(e^{i\omega})\right|}, \text{ for } \omega\in[-\pi,\pi],$$

or,

$$|\xi^*(\omega)| \leq \frac{1}{1+|\eta^*(\omega)|\left|\hat{P}^{-1}(e^{i\omega})\right|\left|\bar{P}(e^{i\omega})\right|}, \text{ for } \omega\in[-\pi,\pi].$$

Therefore, we can define a new, robust Q-filter with

$$\xi^*_r(\omega) = \min\left\{\xi^*(\omega), \frac{1}{1+|\eta^*(\omega)|\left|\hat{P}^{-1}(e^{i\omega})\right|\left|\bar{P}(e^{i\omega})\right|}\right\}. \tag{29}$$

B. Finite Horizon

In all real implementations of ILC, the time horizon is finite. For finite time horizon, we approximate the spectrum of *d* using its Fourier Transform and scaling by the iteration length *N* as,

$$\Phi^N_d(\omega) = \frac{1}{N}\left|\sum_{k=0}^{N-1} d(k)e^{-\frac{i\omega k}{N}}\right|^2. \tag{30}$$

The optimal filters are then constructed by replacing

$\Phi_d(\omega)$ with $\Phi_d^N(\omega)$ in (24) and (25).

C. Filter Construction

The optimal Q and L filters may be difficult or impossible to construct to exactly meet the optimal specifications, (24) and (25). Two problems arise: the construction of a zero-phase filter and optimally selecting a filter who spectrum best matches the optimal spectrum. We present one solution to the former problem in Section VI using the so-called *filtfilt* technique. The latter problem is the optimal model fitting problem for which extensive results are available in the field of system identification [13].

D. Simple Design Guidelines

In some applications it may not be cost-effective to develop accurate noise and disturbance spectra models for optimally shaping learning and Q-filters. For these applications we distill the results in the Section IV into simple design guidelines based on an approximate or assumed deterministic-to-stochastic ratio (DSR), $\Phi_d(\omega)/\left(\Phi_w(\omega)+\Phi_v(\omega)\right)$.

Large DSR

At frequencies where stochastic noise is very small, there is no penalty to fast, unfiltered learning. Thus, for large DSR, we should have $\xi^*(\omega)=1$ and $\eta^*(\omega)=1$.

Small DSR

At frequencies where deterministic error is very small, there is little advantage to learning, so we should set $\xi^*(\omega)\approx 0$ or $\eta^*(\omega)\approx 0$. The advantage to setting $\eta^*(\omega)\approx 0$ and keeping $\xi^*(\omega)\approx 1$ is that the deterministic error will eventually be learned (although very slowly). The advantage to setting $\xi^*(\omega)\approx 0$ is the improved robustness this offers (see Section V.A).

The above guidelines are frequency-dependent and the designer may shape $\xi(\omega)$ and $\eta(\omega)$ as DSR changes in different frequency bands. For example, for the illustration in Figure 4.a, the designer may shape $\xi(\omega)$ and $\eta(\omega)$ as in Figure 4.b. This example results in the familiar model-inversion learning with lowpass Q-filter [9],[12].

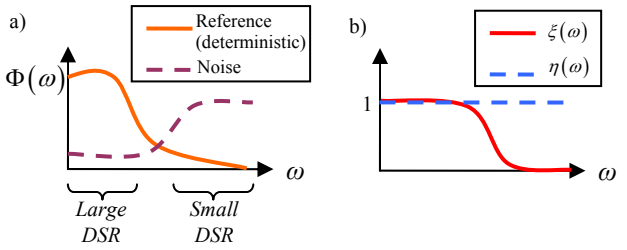

Fig. 4. Illustration of simple design guidelines. a) Estimated DSR. b) Filter design.

E. Coordinated Feedback and ILC Design

A possibility not considered in the optimization is coordinated design of the feedback controller with the ILC. The analysis in Section IV was based on the optimal design for the given disturbance and noise spectra $\Phi_w(\omega)$ and $\Phi_v(\omega)$, but feedback controller design has the possibility to shape those spectra. Thus, a coordinated design strategy might involve designing the feedback controller to mitigate $\Phi_w(\omega)$ and $\Phi_v(\omega)$, especially at frequencies where deterministic disturbances are large. A similar approach is examined in more detail in [14].

VI. Simulation Example

In this section we demonstrate the derived results in a simulation example. The plant is given by $P(\mathrm{q})=0.5\mathrm{q}/(\mathrm{q}-0.5)$, and deterministic error is the pulse given by $d(k)=step(k-100)-step(k-200)$, where $step(k)\triangleq\{1,\ k\geq 1;\ 0,\ o.w.\}$. Noise with variance 0.01 and colored by the highpass filter $F_v(\mathrm{q})=(\mathrm{q}-0.9)/(\mathrm{q}-0.7)$ is added to the measurement signal and disturbances are set to zero, $w_j(k)=0$. Thus,

$$\Phi_v(\omega)=0.01\cdot\frac{1.81-1.8\cos(\omega)}{1.49-1.4\cos(\omega)} \text{ and } \Phi_w(\omega)=0.$$

The time horizon is selected as N=300. The power spectrum for $\hat{e}_0$ is approximated by (30) and shown, along with $\Phi_v(\omega)$, in Figure 5. The learning function is given by $L(\mathrm{q})=\eta(\mathrm{q})(\mathrm{q}-0.5)/0.5\mathrm{q}$.

A fast convergence rate, $\bar{\gamma}=0$, and a slow convergence rate, $\bar{\gamma}=0.95$ are selected for comparison. Optimal η^* and ξ^* are calculated from (24) and (25), respectively, and shown in Figure 6 for $\bar{\gamma}=0$ and in Figure 7 for $\bar{\gamma}=0.95$.

We now construct filters that approximate the optimal η^* and ξ^* figures 6 and 7. Our filters will need to have zero-phase, which can be emulated by using the *filtfilt* technique [15] with a nonzero-phase filter. The *filtfilt* process is given by the following steps

1. The signal is filtered with the nonzero-phase filter, adding phase lag.
2. The result is reversed in time and filtered again with the nonzero-phase filter, removing the phase lag.
3. The result is again reversed in time.

The resultant operation has zero phase and the square of the nonzero-phase filter's magnitude spectrum. Therefore, we are interested in finding filters (with nonzero-phase) whose squared magnitude spectrum approximates the power spectrums in figures 6 and 7. The following filters are obtained and the square of their magnitude spectrum is

plotted in figures 6 and 7. For $\bar{\gamma}=0$, we have $\eta_{fit}^{0}(\mathrm{q})=1$ and $\xi_{fit}^{0}(\mathrm{q})=0.5\mathrm{q}/(\mathrm{q}-0.5)$. For $\bar{\gamma}=0.95$, we have $\eta_{fit}^{0.95}(\mathrm{q})=(0.2536\mathrm{q}-0.030432)/(0.88\mathrm{q}-0.176)$ and $\xi_{fit}^{0.95}(\mathrm{q})=(0.9\mathrm{q}-0.81)/(0.91\mathrm{q}-0.091)$. The approximated filters obtained here are intended for illustrative purposes and do not represent optimal fits.

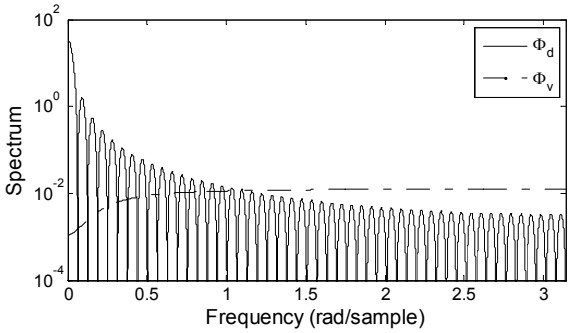

Fig. 5. Spectrum of d and v.

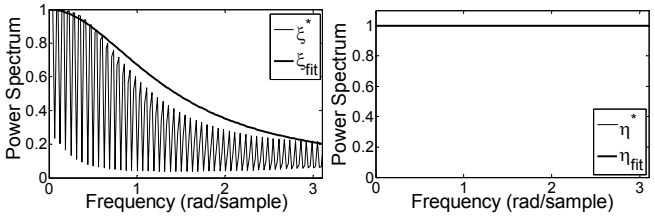

Fig. 6. Filter approximations for $\bar{\gamma}=0$.

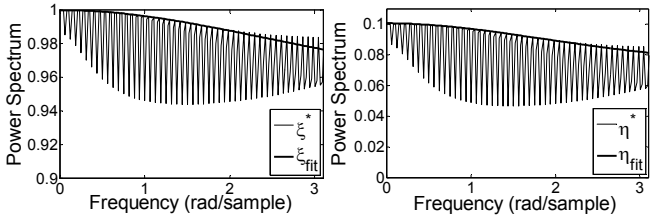

Fig. 7. Filter approximations for $\bar{\gamma}=0.95$.

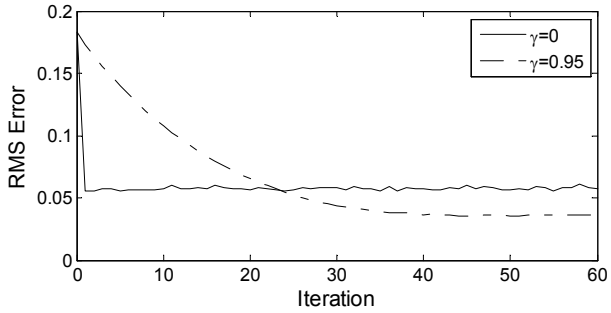

Fig. 8. Convergence behavior.

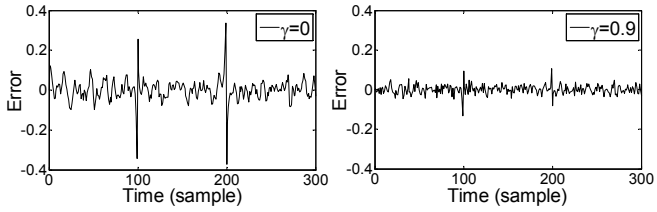

Fig. 9. Error on the 60th iteration.

The convergence of the error rms is shown in Figure 5 and Figure 6 shows the error on the 60th iteration. These results illustrate that slower convergence rates can be used effectively to decrease the converged error.

VII. Conclusions

In this paper we have developed frequency-domain results for ILC systems with mixed deterministic and stochastic disturbances. Optimal filter design based on these results were obtained and demonstrated a fundamental tradeoff between convergence rate and converged performance. Several extensions were considered including robust design and finite-horizon design. For applications where explicit models of the disturbance and noise spectra may not be available, simple design guidelines were presented. Finally, a numerical example demonstrating an application of the optimal design was presented. The example illustrated the converged result versus converged performance tradeoff.

References

[1] Moore, K.L., Iterative Learning Control for Deterministic Systems, Springer-Verlag, 1993.

[2] Bien, Z. and J.-X. Xu, Iterative Learning Control: Analysis, Design, Integration and Applications, Kluwer Academic Publishers, 1998.

[3] Bristow, D.A., M. Tharayil, and A.G. Alleyne, "A Survey of Iterative Learning Control," *IEEE Control Systems Magazine*, vol. 26, no. 3, pp. 96-114, 2006.

[4] Saab, S.S., "A Discrete-Time Stochastic Learning Control Algorithm," *IEEE Trans. on Automatic Control*, vol. 46, no. 6, pp. 877-887, 2001.

[5] Saab, S.S., "On a Discrete-Time Stochastic Learning Control Algorithm," *IEEE Trans. on Automatic Control*, vol. 46, no. 8, pp. 1333-1336, 2001.

[6] Saab, S.S., "Stochastic P-Type/D-Type Iterative Learning Control Algorithms," *International J. of Control*, vol. 76, no. 2, pp. 139-148, 2003.

[7] Saab, S.S., "Optimal Selection of the Forgetting Matrix into an Iterative Learning Control Algorithm," *IEEE Trans. on Automatic Control*, vol. 50, no. 12, pp. 2039-43, 2005.

[8] Norrlof, M. and S. Gunnarsson, "Time and Frequency Domain Convergence Properties in Iterative Learning Control," *International J. of Control*, vol. 75, no. 14, pp. 1114-1126, 2002.

[9] Longman, R.W., "Iterative Learning Control and Repetitive Control for Engineering Practice," *International J. of Control*, vol. 73, no. 10, pp. 930-954, 2000.

[10] Elci, H., R.W. Longman, M. Phan, J.-N. Juang, and R. Ugoletti, "Discrete Frequency Based Learning Control for Precision Motion Control," *Proc. of the IEEE International Conf. on Systems, Man and Cybernetics,* 1994, pp. 2767-2773.

[11] ___ "Simple Learning Control Made Practical by Zero-Phase Filtering: Applications to Robotics," *IEEE Trans. on Circuits and Systems I: Fundamental Theory and Applications*, vol. 49, no. 6, pp. 753-67, 2002.

[12] Kavli, T., "Frequency Domain Synthesis of Trajectory Learning Controllers for Robot Manipulators," *J. of Robotic Systems*, vol. 9, no. 5, pp. 663-680, 1992.

[13] Leonart Ljung, System Identification: Theory for the User, Prentice Hall, 1999.

[14] Helfrich, B.E., *et. al.*, "A Framework for Combined H-Infinity and Iterative Leraning Control Design with Application to Nanopositioning Systems," *to appear American Control Conf.*, 2008.

[15] Gustafsson, F., "Determining the Initial States in Forward-Backward Filtering," *IEEE Trans. on Signal Processing*, vol. 44, no. 4, pp. 988-92, 1996.